Current Research in Food Science 6 (2023) 100433

Contents lists available at ScienceDirect

Current Research in Food Science

journal homepage: www.sciencedirect.com/journal/current-research-in-food-science

The role of glycosylation in amyloid fibril formation of bovine κ-casein

Barana Hewa Nadugala [a,b], Rick Hantink [b,1], Tom Nebl [c], Jacinta White [d], Charles N. Pagel [e], C.S. Ranadheera [a,*], Amy Logan [b,**], Jared K. Raynes [f]

[a] School of Agriculture and Food, Faculty of Veterinary and Agricultural Sciences, University of Melbourne, VIC, 3052, Australia
[b] CSIRO Agriculture and Food, Werribee Victoria, 3030, Australia
[c] Biology Group, Biomedical Manufacturing Program, CSIRO, Bayview Ave/Research Way, Clayton, VIC, 3168, Australia
[d] CSIRO Manufacturing, Bayview Avenue, Clayton, VIC, 3168, Australia
[e] Melbourne Veterinary School, Faculty of Veterinary and Agricultural Sciences, The University of Melbourne, VIC, 3052, Australia
[f] School of Chemical and Biomolecular Engineering, Faculty of Engineering, The University of Sydney, NSW, 2006, Australia

ARTICLE INFO

Handling Editor: Dr. Xing Chen

Keywords:
Genetic variant
Glycan
Self-assembled
Micelle-like aggregate
Protein aggregation

ABSTRACT

In order to explore the functions of glycosylation of κ-Casein (κ-CN) in bovine milk, unglycosylated (UG) and twice glycosylated (2G) forms of κ-CN B were purified by selective precipitation followed by anion exchange chromatography from κ-CN BB milk and tested for their amyloid fibril formation and morphology, oligomerisation states and protein structure. The diameter of self-assembled κ-CN B aggregates of both glyco-form were shown for the first time to be in the same 26.0–28.7 nm range for a 1 mg mL^{-1} solution. The presence of two bound glycans in the protein structure of 2G κ-CN B led to a greater increase in the maximum amyloid fibril formation rate with increasing protein concentration and a difference in both length (82.0 ± 29.9 vs 50.3 ± 13.7 nm) and width (8.6 ± 2.1 vs 13.9 ± 2.5 nm) for fibril morphology compared to UG κ-CN B. The present results suggest that amyloid fibril formation proceeds at a slow but steady rate via the self-assembly of dissociated, monomeric κ-CN B proteins at concentrations of 0.22–0.44 mg mL^{-1}. However amyloid fibril formation proceeds more rapidly via the assembly of either aggregated κ-CN present in a micelle-like form or dissociated monomeric κ-CN, packed into reorganised formational structures above the critical micellar concentration to form fibrils of differing width. The degree of glycosylation has no effect on the polarity of the adjacent environment, nor non-covalent and disulphide interactions between protein molecules when in the native form. Yet glycosylation can influence protein folding patterns of κ-CN B leading to a reduced tryptophan intrinsic fluorescence intensity for 2G compared to UG κ-CN B. These results demonstrate that glycosylation plays an important role in the modulation of aggregation states of κ-CN and contributes to a better understanding of the role of glycosylation in the formation of amyloid fibrils from intrinsically disordered proteins.

1. Introduction

Amyloid fibrils are ordered, unbranched and insoluble protein structures (Wetzel, 2013), formed by the lateral hydrogen bonding of peptides and proteins to form an elongated β-sheet secondary pleated structure (Dobson, 2003) that tend to be around 10 nm in diameter and can grow into the micrometer range (Segers-Nolten et al., 2011). Currently, more than 35 human proteins have been identified with potential to form amyloid-like fibrils (Sipe et al., 2016), with amyloid fibril formation discovered to be a generic property of most polypeptides under certain conditions (Dobson, 2003). The mechanism behind amyloid fibril formation and substances that decrease or prevent this process have gained much interest in recent years as amyloidosis, a physiological condition associated with the development of amyloid fibrils, is classified as the root of over 30 human diseases including type 2 diabetes and some neurodegenerative diseases e.g. Alzheimer's, Parkinson's and Huntington (Chiti and Dobson, 2006; Wetzel, 2013). Moreover, amyloid-like fibril formation has been recently recognised to adversely affect the food processability and shelf life of food products, i.e. age gelation in ultra-high temperature treated bovine milk (Raynes et al.,

* Corresponding author.
** Corresponding author.
E-mail addresses: Senaka.Ranadheera@unimelb.edu.au (C.S. Ranadheera), Amy.Logan@csiro.au (A. Logan).
[1] Deceased.

https://doi.org/10.1016/j.crfs.2023.100433
Received 29 September 2022; Received in revised form 8 December 2022; Accepted 2 January 2023
Available online 3 January 2023

2018). Although it is critical to uncover the mechanism and factors that naturally regulate fibril formation to find solutions to prevent or control protein aggregation in both the medical and food production sectors, it is not yet fully understood.

Bovine milk contains a heterogeneous protein mix which largely (approx. 90% w/w) consists of six major milk proteins identified as α_{s1}-casein (α_{s1}-CN), α_{s2}-casein (α_{s2}-CN), β-casein (β-CN), κ-CN, α-lactalbumin, and β-lactoglobulin. Caseins form a supramolecular structure termed a 'casein micelle' to transport calcium and phosphate to the neonate (Holt et al., 2013), and κ-CN is widely recognised as the protein which creates the outer layer of the micelle and provides steric and electrostatic repulsion between micelles to prevent aggregation (De Kruif, 1998; Horne, 2003; Walstra, 1999; Waugh, 1958).

κ-CN is 169 amino acids in length, containing one tryptophan residue and belongs to the intrinsically disordered protein family that lacks an ordered tertiary structure (Farrell et al., 2004; Farrell et al., 2003). There are 14 κ-CN genetic variants that have been identified so far and the amino acid sequence for the κ-CN variants reported herein are described in Hewa Nadugala et al. (2022). The κ-CN A and B variants are the predominant genetic variants of dairy cattle. The κ-CN A and B allele of A and B genetic variants can be present as homozygous (AA or BB) or heterozygous (AB). κ-CN B differs from κ-CN A at position 136 and 148 with a non-polar isoleucine instead of an uncharged polar threonine at position 136 and a non-polar alanine instead of the negatively charge aspartic acid at position 148 (Farrell et al., 2004; Mercier et al., 1973). κ-CN is the only bovine casein which contains both phosphorylation and glycosylation as posttranslational modifications (O'Riordan et al., 2014) which further contributes to the heterogeneity of κ-CN. There are four potential phosphorylation sites at Ser^{127}, Thr^{145}, Ser^{149} and Ser^{166} (Hernández-Hernández et al., 2011; Holland et al., 2006) and five potential O-glycosylation sites at Thr^{121}, Thr^{131} Thr^{133}, Thr^{142} and Thr^{165} (Nwosu et al., 2010) confirmed in κ-CN.

Protein glycosylation occurs in the Golgi apparatus and endoplasmic reticulum of the mammary cells via various glycosyltransferases (O'Riordan et al., 2014). There are two forms of glycosylation of proteins in bovine milk. These are O-linked glycosylation, in which a glycan attached to the hydroxyl oxygen of the protein's amino acid side chains and N-linked glycosylation, in which amide side chains of the protein's amino acids carriy the glycans (O'Riordan et al., 2014). While the majority of the glycans are tetrasaccharides containing galactose, N-acetylgalactosamine and N-acetylneuraminic acid, monosaccharide, disaccharide and trisaccharide glycan forms are also found (Saito and Itoh, 1992). The degree of glycosylation, or number of attached glycans, is known to affect technologically and economically important functional properties of milk, such as total protein content, casein micelle size and rennetability (Bonfatti et al., 2014; Jensen et al., 2012, 2015). The role of glycosylation of κ-casein (κ-CN), a major milk protein, in cow's milk is currently unknown, although glycosylation is thought to assist in the correct folding of proteins, secretion of proteins in their active confirmation, protecting proteins from digestion, as well as facilitating receptor-ligand interactions, communication and host-pathogen interactions (O'Riordan et al., 2014).

Purified κ-CN in its native form tends to form intermolecular disulphide bonds that may oligomerise into multimers, ranging from dimers to decamers (Rasmussen et al., 1992). These multimers tends to associate further via non-covalent interactions and form micelle-like aggregate oligomers (Farrell et al., 1996) beyond its critical micelle concentration of 0.5 mg mL^{-1} (Ecroyd et al., 2010).

Susceptibility of a peptide or protein to form amyloid fibrils varies with its amino acid sequence, net charge, hydrophobicity and stability of the secondary structure (Sunde et al., 1997). While some models have been proposed i.e. the domain swapping model (Schlunegger et al., 1997) and polar zipper model (Perutz et al., 1994) to explain the amyloid fibril formation process, there are no commonly agreed mechanisms. Generally, the amyloid fibril formation reaction is believed to be initiated with a lag phase (*in vitro*) followed by a rapid growth phase (Chiti and Dobson, 2006; Hamada and Dobson, 2002; Krebs et al., 2004). This lag phase is commonly identified as the nucleation stage which creates colloidal assembly afterwards (Wetzel, 2013). While a lag phase is common for amyloid fibril formation for most proteins, it is not observed for κ-CN due to being an intrinsically disordered proteins that does not need to unfold prior (Ecroyd et al., 2008).

Glycosylation is hypothesised to regulate amyloid fibril formation in intrinsically disordered proteins as it can influence the net charge, size, hydrophobicity and protein-protein interactions of a protein (Broncel et al., 2010; Schedin-Weiss et al., 2014). In this study, the role of glycosylation in amyloid fibril formation was investigated using cow's milk of known κ-CN genetic variants (κ-CN BB) purified to isolate the unglycosylated (UG) κ-CN B and twice glycosylated (2G) κ-CN B forms. To the authors knowledge, this study is the first to investigate the effect of glycosylation on amyloid fibril formation mechanisms in native κ-CN B, excluding the effect of amino acid sequence differences that can be imposed through genetic variants. Moreover, the size of self-assembled native κ-CN B aggregates is reported for the first time.

2. Material and methods

2.1. Materials

2.1.1. Milk

Morning milk samples (2L) were collected and pooled from two individual Australian Holstein Friesian cows of known κ-CN genetics and housed at the Agriculture Victoria Research Centre (Ellinbank, Victoria, Australia; latitude 38°14′S, longitude 145°56′E). Samples were kept cool on ice during transportation (approx. 3 hrs.) and stored under refrigerated conditions at 4 °C once back at the laboratory for processing the following day.

2.1.2. Chemicals

All chemicals were analytical grade or higher grade than analytical grade, purchased from Sigma-Aldrich (St. Louis, MO) unless otherwise stated.

2.2. Methods

2.2.1. Milk treatment

Firstly, milk fat was separated from the serum phase via centrifugation (3000×*g* for 30 min at 3 °C) using a Beckman Coulter J6-MI Centrifuge (Gladesville, Australia). The resulting fat layer was manually lifted from the surface, and the serum filtered through glass wool at 4 °C. The milk serum was subsequently heated (20 °C) and remaining milk fat visible on the surface removed using vacuum suction. Sodium azide (0.02% (w/w)) was added to the serum to prevent microbial growth.

2.2.2. Protein purification

Primary protein purification was performed according to the method of Hill (1963) on two separate occasions (P1 and P2), with some minor adjustments. In short, the casein fraction was removed from the milk serum using a process of acid precipitation where the serum was acidified to the isoelectric point of casein (pH 4.6) using 4M HCl. The precipitate (curd) was collected, washed using deionised water and compressed using a nylon cloth. The compressed curd was suspended in deionised water (3 L) and the pH adjusted to 7.0 using 4M NaOH and stirred using a high-speed mixer (Ultraturrax T25, ex. IKA© Labortechnik, Germany) set at approx. 9000 RPM overnight under refrigerated conditions (4 °C). The process of precipitation and resuspension was repeated a further two times on each occasion, with deionised water (1.3 L) used in the last step.

An aliquot of 4 M $CaCl_2$ was added to the final casein suspension to reach a molarity of 0.266 M to precipitate the calcium-sensitive caseins (i.e. α_{s1}-CN, α_{s2}-CN and β-CN). After keeping the sample solution at 4 °C

for 1 h, the suspension was gradually heated to 35 °C in a water bath and centrifuged using a Beckman Coulter J6-MI Centrifuge (4000 *g* for 15 min at room temperature) equipped with a JS-4.2 Rotor. The supernatant was separated and dialysed against 40 L of deionised water using a 10 kDa molecular weight cutoff (MWCO) cellulose dialysis membrane (Spectrum city, NJ, USA) to remove calcium, chloride and sodium ions added to the milk through the purification steps. The dialysed samples were frozen to −80 °C and freeze-dried using a VirTis Genesis freeze dryer (SP Industries, PA, USA) to concentrate purified fractions by removing excess moisture without denaturing protein. The freeze-dried sample was subsequently stored at −22 °C awaiting secondary processing.

Kappa-casein glycovariants were separated and collected using anion exchange chromatography according to the protocol developed by Vreeman et al. (1986). An ÄKTA PURE fast protein liquid chromatography system (FPLC) (GE Healthcare Biosciences, Uppsala, Sweden) equipped with a F9–C fraction collector and operated using the UNICORN™ software package was used. An aliquot of freeze dried primary purified sample (500 mg) was dissolved in Solvent A (3.3 M urea, 20 mM Tris base, 20 mM DL-dithiothreitol, pH 8.0) to unfold and increase the net negative charge of the proteins and filtered through a 0.45 μm filter before loaded on to a HiPrep™ Q High Performance 16/10 (20 mL) column (GE Healthcare, Uppsala, Sweden) packed with Q-sepharose resin (Global Life Sciences Solutions, MA, USA). Solvent A with 1 M NaCl was used as the wash buffer (Solvent B) in a ratio of 100:00, 79:21, 0:100 and 100:00 of Solvent A to B at 1.0 mL min^{-1} to gradually increase conductivity of the column, which led to the release of bound protein based on net negative charge.

Fractions corresponding to peaks of interest were collected and verified. 20 mM DL-dithiothreitol was added to the verified fractions to inhibit disulphide bond formation, and subsequently dialysed individually using 10 kDa MWCO cellulose dialysis cassettes (Thermo Fisher Scientific, MA, USA) against deionised water (40 L) at 4 °C. Dialysis buffer changing frequency was 1h, 5h and overnight. Dialysed samples were frozen (−80 °C), freeze dried and stored (−22 °C) as described earlier. Secondary purification was performed on three separate occasions (once using P1 primary purified sample and twice from P2) to generate three sample sets (n = 3).

2.2.3. Fraction verification

Reverse phase-HPLC was used to identify genetic variants and confirm purity of the collected fractions as described previously (Bobe et al., 1998; Bonfatti et al., 2008; Bordin et al., 2001). In short, a reversed-phase C-18 column (250 × 4.6 mm) with 300 Å pore diameter and 5 μm particle size (Jupiter®, Phenomenex Inc, CA, USA) was used in a Dionex UltiMate 3000 chromatographic system (Thermo Fisher Scientific, MA USA), with the following linear gradient of Solvent C and D respectively: 29.7–37.0% (25 min), 37.0–45.0% (23 min), 45.0–62.4% (2 min), and 62.4%–29.7% (5 min) at a flow-rate of 0.700 mL min^{-1}; where Solvent C is composed of 0.1% trifluoroacetic acid in ultrapure water and Solvent D of 9.9% water and 0.1% TFA in acetonitrile. The column temperature was kept at 40 °C.

Electrospray ionisation quadruple time-of-flight mass spectrometry (ESI-Q-TOF-MS) was carried out on an UltiMate 3000 HPLC system (Thermo Fisher Scientific) coupled to a MaXis II Q-TOF mass spectrometer (Bruker Daltonics, MA USA) to identify the degree of glycosylation. In short, the purified samples (1 mg mL^{-1}) in H_2O were diluted with 0.1% formic acid and loaded onto a 50 × 4.6 mm, 5 μM particle size, 300 Å pore size Agilent PLRP-S column (Agilent) pre-equilibrated with 0.1% formic acid. The protein was eluted from the column at a flow rate of 250 μL min^{-1} by applying a linear 30 min gradient from 0 to 80% mobile phase B (mobile phase A: 0.1% (v/v) formic acid; mobile phase B: 90% (v/v) acetonitrile/0.1% (v/v) formic acid) and ionised using an Apollo II electron spray ion source (Bruker Daltonics) with nebulizer pressure set at 1.8 Bar and dry gas maintained at 220 °C at a flow rate of 8L min^{-1}. High-resolution LC-MS data were analysed using the Intact Mass parsimonious charge-state deconvolution algorithm (Bern et al., 2018). Casein genetic variants and the number of glycosylated and phosphorylated residues were identified based on the molecular weights reported by Day et al. (2015); Vincent et al. (2016).

2.2.4. Sample preparation for the further experiments

Approximately 5 mg of each glycovariant sample was suspended in sodium phosphate buffer (1 mL, 50 mM, pH 6.7) and allowed to solubilize overnight at 4 °C. After filtering through a 0.2 μm filter, the protein concentration was confirmed using a ND-1000 UV–Vis spectrophotometer from NanoDrop Technologies (Wilmington, DE) at 280 nm according to the method of Raynes et al. (2017).

2.2.5. Kappa casein self-assembled micelle-like aggregate size determination

The hydrodynamic diameter (D_h) of the self-assembled rehydrated κ-CN glycovariant aggregates were measured at room temperature via dynamic light scattering using a Zetasizer Nano ZS (Malvern Instruments, Malvern, UK) according to the method of Raynes et al. (2015). In short, samples were diluted to 1 mg mL^{-1} using sodium phosphate buffer (50 mM, pH 6.7), filtered through a 0.2 μM syringe filter (Pall Corp., Hauppauge, NY) and analysed in a 1 cm path-length quartz cuvette (Hellma Analytics, Müllheim, Germany) using a fixed detector angle of 173°. The refractive index was set as 1.45 for protein and 1.33 for the solvent phase. The measurement duration was set to automatic and each sample was measured in triplicate on three separate occasions.

2.2.6. Tryptophan intrinsic fluorescence determination for changes in protein structure

Kappa-casein B was solubilized in sodium phosphate buffer (50 mM, pH 6.7) to a concentration of 3.5 mg mL^{-1}. An aliquot (100 μL) of each sample was added to a 96 well flat bottom, non-binding surface black polystyrene microplate (Corning Incorporated, NY, USA) and the tryptophan fluorescence monitored using a Varioskan Flash microplate reader (Thermo Fisher Scientific, MA, USA). Emission spectra were individually recorded over a wavelength range of 310 nm–450 nm in 1 nm initials (100 ms $scan^{-1}$) at an excitation wavelength of 280 nm. Analysis was performed in duplicate for each sample prepared on three separate occasions. Blanks corresponding to the buffer were subtracted to remove background fluorescence. No indicator was used in this analysis.

2.2.7. Transmission electron microscopy

Kappa casein B was solubilized in a sodium phosphate buffer (50 mL, pH 6.7) to a concentration of 0.35 mg mL^{-1}. Microscopy images of solubilized κ-CN B before and after 24 h incubation at 37 °C were captured using transmission electron microscopy (TEM) according to the method of Raynes et al. (2017). In short, to make the carbon film hydrophilic, carbon-coated grids (EMSCF200H-CU-TH, ProSciTech) were glow discharged with a Pelco EasiGlow Glow Discharge unit. A drop (2 μL) of sample was applied to an upturned grid held in anti-capillary forceps, over moist filter paper, and allowed to adsorb for 1 min. Excess liquid was removed with Whatman 541 filter paper before inverting the grid for 30 s onto a drop (30 μL) of phosphotungstic acid stain (2%, pH 6.9) on Parafilm. The grid was removed, and the stain was wiped away with filter paper before viewing under the microscope. The samples were examined with a Tecnai 12 Transmission Electron Microscope (FEI, Eindhoven, The Netherlands) at 120 KV. Images were captured at various magnifications with an FEI Eagle 4kx4k CCD camera and AnalySIS v3.2 camera control software (Olympus). Each grid was systematically examined and a minimum of 5 images captured at a variety of magnifications between 20 and 60,000x to ensure a representative view of the sample. The diameter of the κ-CN B aggregates, and the length and width of the resulting amyloid fibrils were measured using ImageJ software package (National Institutes of Health, US).

2.2.8. Amyloid fibril formation kinetic determination

The rate of amyloid fibril formation was determined according to the method of Raynes et al. (2017) utilizing an *in situ* thioflavin T spectroscopic binding assay. A stock solution for each sample was prepared (3.5 mg mL^{-1}) using a sodium phosphate buffer (50 mM, pH 6.7), diluted further to create a 5x dilution series of 1.75, 0.88, 0.44, 0.22,0.11 and 0.05 mg mL^{-1}. Thioflavin T was added to each sample to a final concentration of 2.5 μM and amyloid fibril formation monitored by measuring the increase in fluorescence of thioflavin T with excitation and emission wavelengths of 450 and 485 nm, respectively. Readings were collected every 10 min for 16 h at 37 °C using a FLUOstar OPTIMA microplate reader (BMG LABTECH, Mount Eliza, AU). Analysis was performed in duplicate for each sample prepared on three separate occasions. Background correction was performed using a florescent reading from a well containing reagents but no sample. The maximum fibril formation rate was measured as the maximum change in thioflavin florescent intensity over a 60 min period for each protein concentration. Data was normalised to the highest maximum fibril formation rate for each data set to directly compare across all assays.

2.2.9. Statistical analysis

The experiment was conducted in triplicate using three independent sample sets and analysis was performed in at least duplicate on each occasion. Results are reported as the average ± the standard deviation. One-way Analysis of variance (ANOVA) was performed using a Minitab statistical software package 19.2020.1 (Minitab Ltd, Coventry, UK) to evaluate the self-assembled micelle-like aggregate size, data generated through the intrinsic fluorescence assay and compare aggregate diameter, amyloid fibril length and width observed in TEM images. The level of significance was considered at $p \leq 0.05$.

3. Results

3.1. Protein purification

A process of precipitation was used to separate the casein and whey proteins of the skimmed milk serum, followed by the selective purification of κ-CN from other caseins present in the milk. Secondary purification via FPLC was conducted to remove impurities and fractionate the κ-CN extract on the basis of net charge, thereby the degree of glycosylation. The identity of the κ-CN variant and purity of the collected fractions was determined using RP-HPLC (Fig. 1), whereas the degree of glycosylation for each collected fraction was identified using ESI-Q-TOF-MS, allowing the selection of fractions of interest for the current study, namely the UG and 2G κ-CN B fractions. The Observed masses of each sample were compared with theoretical molecular masses reported by Day et al. (2015) and Vincent et al. (2016). Reported mass fragments of 2G κ-CN B with 20,941.5 Da and 20,899.0 Da, were identified as κ-CN B (2P) + 2x glycans and κ-CN B (1P) + 2x glycans, respectively where the major peak of UG κ-CN B with 19,002.9 Da was identified as κ-CN B (1P) (Table 1). The purity of the UG κ-CN freeze-dried fractions (on a peak area basis) were 74 ± 3% across P1 and P2, and the corresponding purity of the 2G κ-CN fractions were 81 ± 2%, respectively. The remaining portion of each UG κ-CN B samples consisted of small amounts (less than 3%) of glycosylated κ-CN B and approximately 20% of other caseins while the remaining portion of each 2G κ-CN B samples consisted of approximately 5% unglycosylated κ-CN B, 14% of other glycosylated κ-CN B forms and approximately 3% of other caseins.

3.2. Self-assembled micelle-like aggregate size

Table 2 shows the average D_h of the UG and 2G κ-CN B micelle-like self-assembled aggregates. The average D_h was the same for both the UG and 2G κ-CN B structures, i.e. 27.2 ± 1.5 and 26.9 ± 0.9 nm respectively, indicating that the glycosylation of κ-CN and subsequent

Table 1
The molecular mass of purified twice glycosylated (2G) and unglycosylated (UG) κ-casein B (κ-CN B) glycovariants analysed by liquid chromatography-mass spectrometry (LC-MS). The corresponded reversed phase-HPLC chromatogram can be found in Fig. 1.

Glycosylation level	Observed mass (Da)	Theoretical mass (Da)	Possible Posttranslational Modifications
2G κ-CN B	20,899.0	20,900	κ-CN B (1P) + 2x glycans [a]
UG κ-CN B	19,002.9	19,002	κ-CN B (1P) [a]

[a] Casein genetic variant and the number of glycosylated and phosphorylated (P) residues were identified based on the molecular weight reported by Day et al. (2015).

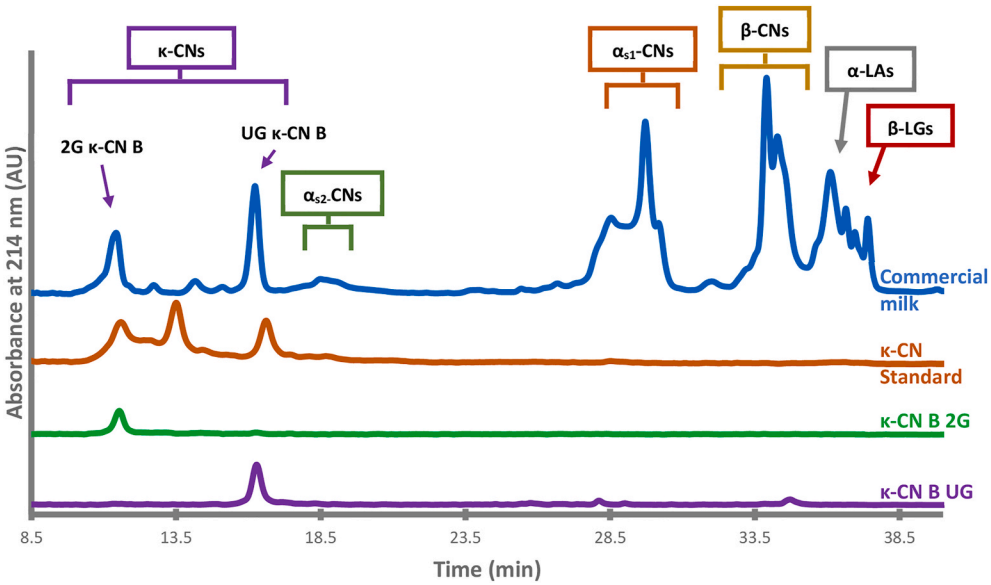

Fig. 1. Example reversed-phase high performance liquid chromatography (RP-HPLC) spectra of twice glycosylated (2G) and unglycosylated (UG) κ-casein B (κ-CN B) used to identify peaks generated through ion exchange. Absorbance is reported as absorbance units (AU).

Table 2
Hydrodynamic diameter (D_h) and the tryptophan intrinsic fluorescence assay λ_{max} and I_{max} for purified twice glycosylated (2G) and unglycosylated (UG) κ-casein B (κ-CN B) glycovariants. Results are the average of three independent sample sets ± the standard deviation. Values within a column that do not share a common superscript letter are significantly different ($p \leq 0.05$).

Glycosylation level	D_h (nm)	Polydispersity Index	λ_{max} (nm)	Normalised I_{max} (AU)
2G κ-CN B	26.9 ± 0.9 [a]	0.36 ± 0.05	327.7 ± 4.0 [a]	70.1 ± 8.1 [a]
UG κ-CN B	27.2 ± 1.5 [a]	0.18 ± 0.04	330.0 ± 3.5 [a]	100 [b]

λ_{max} - wavelength of maximum fluorescence intensity, I_{max} - maximum fluorescence intensity.

inclusion of two bound glycan groups does not influence the overall diameter of its oligomeric quaternary structure. To the best of the authors' knowledge, this is the first time reporting the D_h of self-assembled and purified glycosylated and un-glycosylated κ-CN aggregates in the literature. The size of self-assembled aggregates formed from a different casein protein (β-CN) are noted to be in a similar range (Raynes et al. (2015).

3.3. Tryptophan intrinsic fluorescence emission spectra

The intrinsic fluorescence of aromatic amino acids residues are sensitive to the protein's microenvironment such as polarity and protein folding (Gorinstein et al., 2000; Hellmann and Schneider, 2019). Differences in the maximum fluorescence intensity (I_{max}) and wavelength of maximum fluorescence intensity (λ_{max}) are used to characterise the structural and functional properties of proteins (Vivian and Callis, 2001). Table 2 shows the average λ_{max} and I_{max} of UG and 2G κ-CN B in their native state. The average λ_{max} was the same for both the UG and 2G κ-CN B, i.e. 330.0 ± 3.5 and 327.7 ± 4.0 nm respectively, indicating no difference in environment when exposing the tryptophan residues of either protein to the experimental buffer. This reflects that the level of glycosylation does not influence the polarity of the tryptophan's residue's molecular environment, supported by the dynamic light scattering

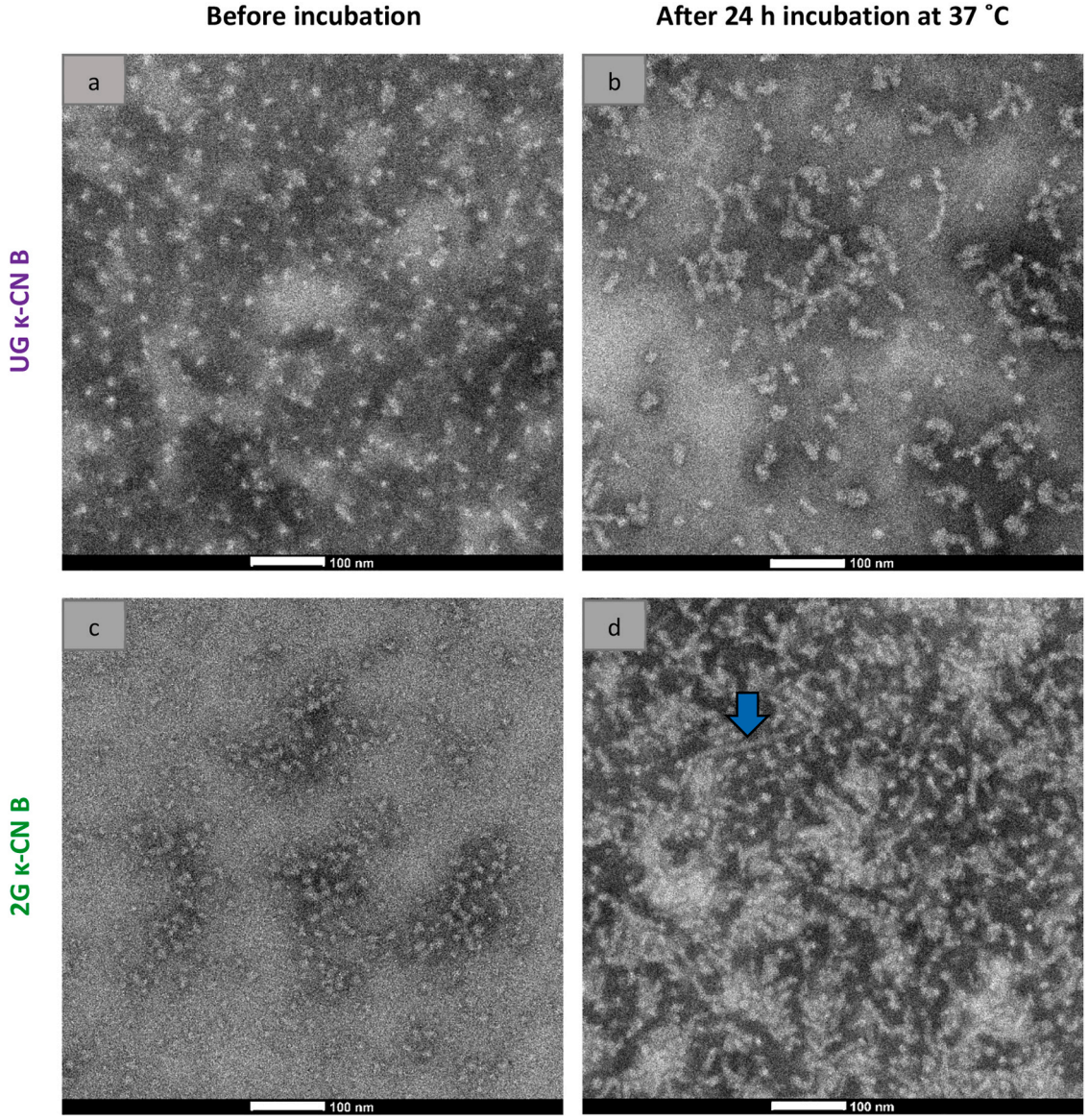

Fig. 2. Transmission electron micrographs of unglycosylated (UG, a and b) and twice glycosylated (2G, c and d) κ-casein B (κ-CN B) before incubation (a and c) and after incubation for 24 h at 37 °C (b and d). Scale bars represents 100 nm magnification. The blue arrow is used to identify an amyloid fibril on image d. (For interpretation of the references to colour in this figure legend, the reader is referred to the Web version of this article.)

results (D_h) which show similar sized self-assembled aggregates at the quaternary structure level (Table 2). Moreover, the λ_{max} indicates that both UG and 2G κ-CN B exhibit an average level of hydrophobicity, where emission maximums from 310 to 350 nm tend to represent the range for very hydrophobic to very polar environments (Hellmann and Schneider, 2019). A decrease in fluorescence intensity was observed between the spectra of 2G compared to UG κ-CN B, where 2G κ-CN B consistently presents a significantly lower I_{max} compared to UG κ-CN B, related to the unfolding of the protein, i.e. opening of the structure due to the inclusion of the negatively charged glycan molecules (Gorinstein et al., 2000).

3.4. Transmission electron microscopy

Fig. 2 (a,b) shows the TEM images of UG and 2G κ-CN B self-assembled aggregates captured prior to incubation. The average aggregate size for UG and 2G κ-CN B measured using ImageJ software was 13.4 ± 2.6 and 13.5 ± 2.2 nm, respectively (Table 3). Similar to the dynamic light scattering results shown in Table 2, the average diameter of aggregates for both the UG and 2G κ-CN B structures was the same as each other, albeit consistently smaller in magnitude than that measured in buffer due to the dehydrated and shrunken nature of the samples processed for TEM imaging. This agrees with Leonil et al. (2008) who observed the same trend for purified κ-CN in their TEM experiment, reporting that both glycosylated and unglycosylated κ-CN formed spherical aggregates around 10–12 nm in diameter, again indicating that glycosylation level does not seem to affect the packing of κ-CN in self-assembled aggregated oligomeric forms.

Fig. 2 (c,d) shows the TEM images of the UG and 2G κ-CN B captured after incubation (24 h, 37 °C) and subsequent amyloid fibril formation. Fibril formation is clearly evident in both samples with the formation of linear aggregate as small as 17.0 nm and as large as 167.5 nm in length. The average length and width of the amyloid fibrils was different between the UG (50.4 ± 15.1 nm in length and 15.4 ± 3.7 nm in width) and 2G (85.7 ± 28.4 nm in length and 8.2 ± 2.0 nm in width) κ-CN B structures, with 2G κ-CN B noted to more closely resemble typical amyloid fibrils reported in the literature, i.e. long, straight, thin and unbranched structures of approximately 10 nm in width that can grow up to several micrometers in length (Rambaran and Serpell, 2008; Segers-Nolten et al., 2011). In comparison, the amyloid fibrils formed in the incubated UG κ-CN B sample appear visibly shorter and wider. While there is little change in the dimension of higher-order structures of UG κ-CN B, there is a significant difference between the diameter and width of aggregates and amyloid fibrils of 2G κ-CN B. This indicates that fibril formation of UG κ-CN B might occur via direct assembly of oligomeric aggregates while fibril formation of 2G κ-CN B most likely occurs via a different mechanism.

3.5. Thioflavin T spectroscopic assay

Thioflavin T is a fluorescent dye that is widely used to monitor the formation of amyloid fibrils as it specifically binds to β-sheet structures and shows fluorescence upon binding (Hudson et al., 2009). The fluorescence intensity of a series of UG and 2G κ-CN B solutions of decreasing protein concentration was measured to investigate amyloid fibril formation kinetics. The *in situ* thioflavin T fluorescence intensity results indicate that amyloid fibril formation occurred for protein concentrations of 0.22 (2G κ-CN B) or 0.44 (UG κ-CN B) mg mL^{-1} and above and almost plateaued thioflavin T fluorescence intensity over more than 12- hr suggest that formed amyloid fibrils are stable and this assemble behaviour is not reversing over time (data not shown). The reaction proceeds immediately upon introduction of the κ-CN substrate to the thioflavin T dye and concurrent temperature increased to 37 °C (Fig. 3). No incubation or lag phase in formation was visible, confirming the findings of others for κ-CN (Ecroyd et al., 2008) and other intrinsically disordered proteins. Moreover, protein concentration dependent differences in initial fluorescence were noted for both UG and 2G κ-CN B, in agreement with Ecroyd et al. (2008), Farrell et al. (2003) and Thorn et al. (2005). These concentration dependent differences in thioflavin T fluorescence were observed to continue over time for both UG and 2G κ-CN B, however the rate of increase reduced and almost plateaued for 2G κ-CN B across all protein concentrations from around the 360 min point onwards, indicating that a rate limiting step for fibril formation was reached based on substrate availability as shown by Ecroyd et al. (2008). In comparison, amyloid fibril formation was observed to proceed at a slow but consistent rate across the entirety of the 16-hr incubation assay for UG κ-CN B protein concentrations of 0.44 mg mL^{-1} and above (Fig. 3).

The maximum amyloid fibril formation rate of UG and 2G κ-CN B as a function of protein concentration is shown in Fig. 4, indicating that the increase in fibril formation rate is linear with respect to κ-CN B concentration. This is consistent with Ecroyd et al. (2010), who found a similar trend at lower protein concentrations. The relative increase in the maximum amyloid fibril formation rate with protein content was significantly higher in 2G compared to UG κ-CN B for concentrations above the critical micelle concentration, (i.e. > 0.5 mg mL^{-1}).

Table 3
Diameter of self-assembled micelle-like aggregates of purified twice glycosylated (2G) and unglycosylated (UG) κ-casein B (κ-CN B) glycovariants before incubation, and amyloid fibril length and width after 24 h incubation at 37 °C calculated from TEM images (Fig. 2). Results represent the average size of the non-heat-treated aggregates or incubated fibrils measured across 5-7images per sample ± the standard deviation. Values within a column that do not share a common superscript lowercase letter are significantly different ($p \leq 0.05$). Values within a row that do not share a common superscript uppercase letter are significantly different ($p \leq 0.05$).

Glycosylation level	Diameter of aggregates (nm)	Amyloid fibril length (nm)	Amyloid fibril width (nm)
2G κ-CN B	13.5 ± 2.2 ^{a,B}	85.7 ± 28.4 ^{a,C}	8.2 ± 2.0 ^{a,A}
UG κ-CN B	13.4 ± 2.6 ^{a,A}	50.4 ± 15.1 ^{b,B}	15.4 ± 3.7 ^{b,A}

4. Discussion

It is known that κ-CN has a tendency to assemble into amyloid fibrils, similar to most other unfolded proteins, however follows alternative aggregation pathway to safely and efficiently transport nutritious milk to the neonate without amyloid fibril formation, which may otherwise aggregate and block the mammary ducts (Holt et al., 2013; Leonil et al., 2008). The major finding of this study was that amyloid fibril formation was significantly higher in 2G κ-CN B, while fibril formation rate of UG κ-CN B appears to be significantly lower.

The current study has utilised native, unreduced κ-CN while most other studies designed to examine κ-CN amyloid fibril formation have used reduced carboxymethylated forms of κ-CN (Ecroyd et al., 2008; Leonil et al., 2008). Moreover, one purified genetic variant of κ-CN (κ-CN B) (Fig. 5) is utilised herein, and the current study compares one single glycosylation form to another glycosylation form (i.e. UG compared to 2G). This has allowed for the effect of glycosylation to be studied in isolation, without the influence of other variables, such as changes in polarity and net charge introduced when multiple genetic variants are present.

The maximum amyloid fibril formation rate for 2G and UG κ-CN as a function of protein concentration is shown in Fig. 4c. The results demonstrate that isolated κ-CN, regardless of the glyco-form, is capable of forming amyloid fibrils at a concentration of 0.22–0.44 mg mL-L, which is below the critical micelle concentration of κ-CN, previously reported as 0.5 mg mL-1 (Ecroyd et al., 2010). This shows that dissociated forms of κ-CN are able to elongate and form a linear β-sheet secondary fibril structure at lower concentrations, albeit at a much slower rate. However, noting that amyloid fibril formation did not occur in the very low protein concentration systems (i.e. 0.05 and 0.11 mg

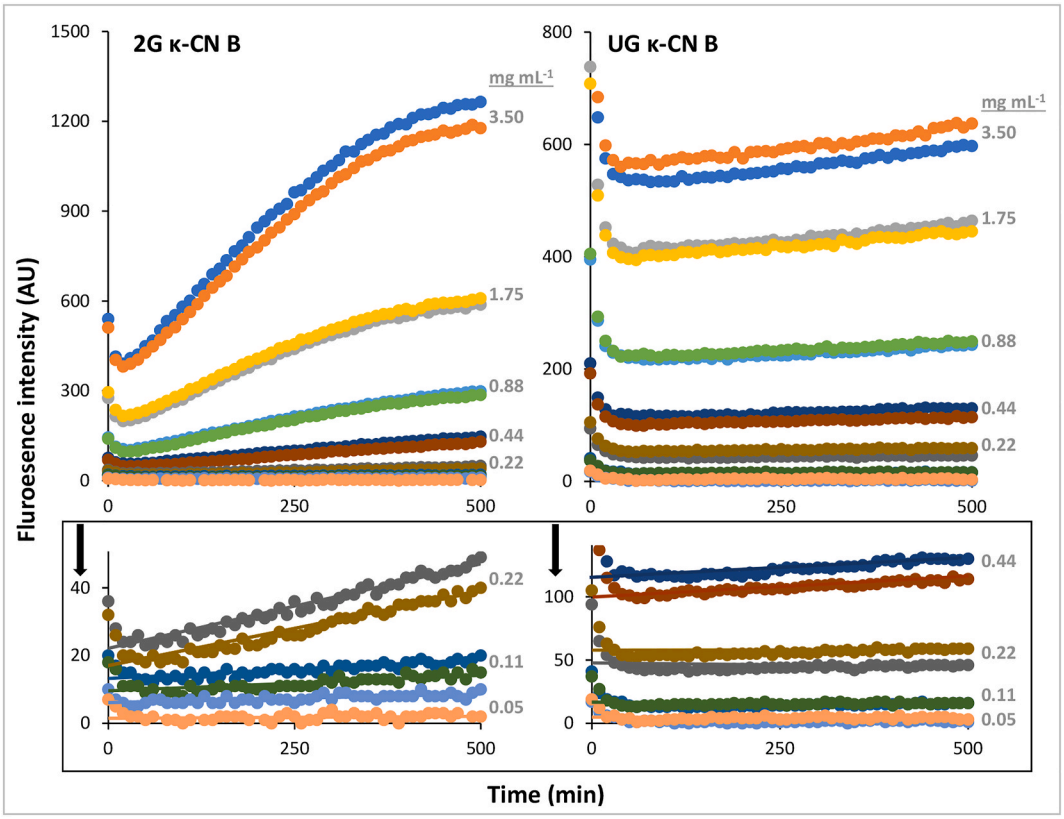

Fig. 3. Duplicate analysis for thioflavin T fluorescence intensity (AU) of (left top) twice glycosylated (2G) and (right top) unglycosylated (UG) κ-casein B of increasing concentration (0.05–3.50 mg mL^{-1}) over time (min) on one of the three occasions. Bottom images present the same analysis, zoomed in on the y-axis to better demonstrate fibril formation for the lower concentration samples.

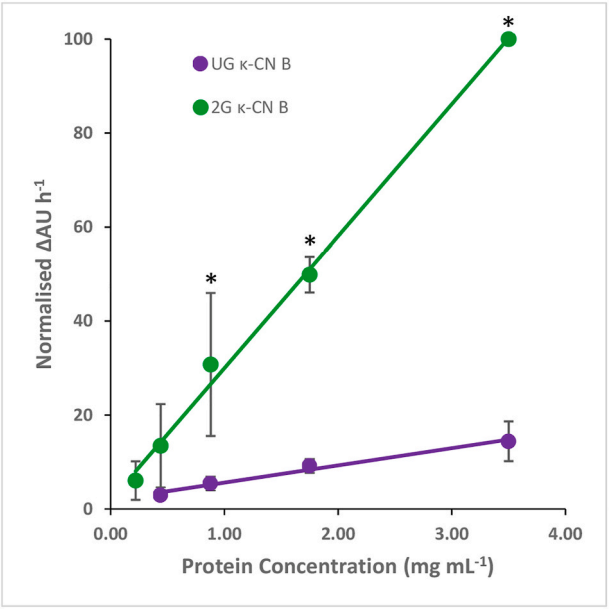

Fig. 4. Maximum amyloid fibril formation rate of twice glycosylated (2G) and unglycosylated (UG) κ-casein B (κ-CN B) as a function of protein concentration. * Shows significantly difference ($p \leq 0.05$) based on one-way Analysis of variance (ANOVA) conducted using three independent and normalised sample sets and at least duplicate analysis on each occasion.

mL-1). Amyloid fibril formation below the critical micelle concentration of κ-CN is in agreement with Ecroyd et al. (2010), who also observed the formation of amyloid fibrils from disassociated forms of κ-CN. However, protein concentrations below 0.25 mg mL-1 were not examined in their work and a lower level cut off for fibril formation was subsequently not established.

A similar increase in the maximum formation rate for both glycoforms with protein content below the critical micelle concentration, indicates that glycan attachment has no effect on amyloid fibril formation in 2G and UG κ-CN when present in a dissociated and un-aggregated form (Fig. 4). However, the relative increase in the maximum amyloid fibril formation rate of κ-CN 2G was markedly higher than that of κ-CN UG for solutions prepared at a concentration of 0.88 mg mL-1 and above. This indicates that differences in the organisation or packing of the different κ-CN self-assembled aggregates with and without attached glycans led to significant differences in the rate of amyloid fibril formation above the critical micelle concentration, demonstrating that glycosylation increases amyloid fibril formation susceptibility of κ-CN when existing as self-assembled micelle-like aggregates. This is in disagreement with Leonil et al. (2008) who reported a higher fibril formation rate for UG κ-CN compared to glycosylated κ-CN, after studying amyloid fibril formation of carboxymethylated κ-CN. This might be a result of conformation difference attributed to the inclusion of non-separated κ-CN (i.e. both B and A genetic variants likely present) in the work of Leonil et al. (2008) compared to the study herein that is specific for κ-CN B, indicating that amyloid fibril formation kinetics may differ for κ-CN A and have an overriding effect in non-separated κ-CN systems. Another potential explanation for the disparate outcomes is a difference in the number of disulphide bonds caused by the presence or absence of a carboxymethyl group in the κ-CN structure. Carboxymethylation modifies the amino acid side chains that can develop

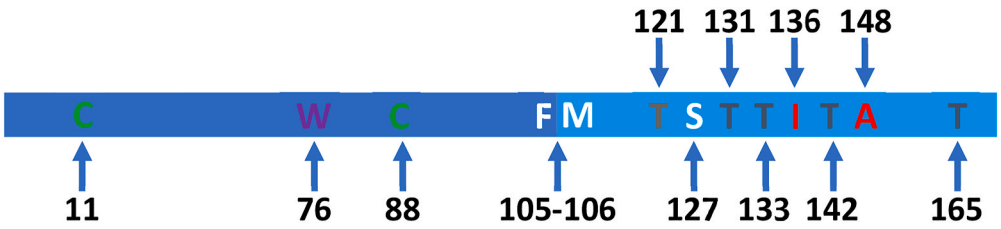

Fig. 5. Potential modification in κ-casein B. This schematic summarises the potential glycosylation sites (T), phosphorylation sites (S), disulphide bond sites (C) and amino acid substitution (I and A) compared to the κ-CN A genetic variant. The dark blue colour represents para-CN and the light blue colour represents the caseinomacropeptide segments of the κ-CN B. The rennet cleavage site is located between the 105 and 106 amino acid residues. Full amino acid sequence and amino acid sequence of other κ-CN genetic variants can be found in Hewa Nadugala et al. (2022). Numbers represent the amino acid residue position in the sequence. (For interpretation of the references to colour in this figure legend, the reader is referred to the Web version of this article.)

disulphide bonds, i.e., cysteine in this case (Hirs, 1967). A significantly higher amyloid fibril formation rate in 2G κ-CN B compared to UG when above the critical micelle concentration, suggests that UG κ-CN B has a higher energy barrier to overcome in order to enable the conversation of oligomeric state of κ-CN to dissociated state. It indicates that the increased net negative charge of the protein due to the addition of two bound glycan molecules, results in weaker non-covalent interaction and disulphide bonds between κ-CN molecules which increases the propensity of releasing disassociated protein forms resulting in a higher tendency to form fibrils.

It is known that glycosylation has an effect on casein micelle size, receptor-ligand interactions, host-pathogen interactions and emulsification of the milk (Bijl et al., 2014; Kreuβ et al., 2009; O'Riordan et al., 2014). Most of these properties are linked with high charge density and hydrophilicity of glycans (Holt et al., 2013), and those properties are important to the functional roles of the milk. Results of the current study shows that glycosylated κ-CN B has a significantly higher rate of amyloid fibril formation than unglycosylated κ-CN B. Although glycosylated κ-CN B may play a role in the functional properties of milk, it seems equally important to transport milk to the neonate without the formation of amyloid fibrils. The results indicate that unglycosylated κ-CN B has a role in the balance between the functional role of κ-CN B and its stability. This might be the reason why UG κ-CN B shows significantly lower amyloid fibril formation compared to 2G κ-CN B under the same condition. This indicates that UG κ-CN B may play a governing role in the control of amyloid fibril formation, limiting the overall reaction rate by balancing the glycosylated to unglycosylated κ-CN ratio in cow's milk. There might be a chaperon action in UG κ-CN B, however, more investigation is needed to make a conclusion.

Though the resulting difference in Imax of glycosylated and unglycosylated κ-CN indicates changes in secondary structures of tested proteins (Gorinstein et al., 2000; Hellmann and Schneider, 2019), the same average λ_{max} indicates that secondary structure difference does not influence the polarity of the tryptophan's adjacent environment (Gorinstein et al., 2000; Hellmann and Schneider, 2019). Moreover, Dh of both UG κ-CN and 2G κ-CN at 1 mg mL-1 were shown to be the same at room temperature, indicating that differences in the intermolecular interactions due to glycosylation had no effect at low temperatures. However, differences in amyloid fibril formation rates between glyco-forms incubated at 37 °C indicate that the changes in intermolecular interactions due to glycosylation can lead to differences when under stress conditions, i.e., when exposed to higher temperatures where the fibril formation reaction is moving to a lower free energy state and where proteins are stabilised in the form of amyloid fibrils.

The TEM micrographs show that both UG and 2G κ-CN B are present as curly and rugged surface linear aggregates, which aligns with Chun et al. (2012) who observed thicker fibrils with a rugged surface using unreduced forms of κ-CN, while Ecroyd et al. (2008), Ecroyd et al. (2010), Leonil et al. (2008), and Pan and Zhong (2015) observed substantially longer fibrils with a smooth surface using reduced forms of κ-CN. Although disulphide bond reduction does not significantly affect the secondary and tertiary structure of κ-CN (Farrell et al., 2003), it is believed that the ability of κ-CN to form oligomers, and the subsequent propensity for amyloid fibril formation, is influenced by changes in the number of disulphide bonds links of cysteine 11 and cysteine 88 (Hewa Nadugala et al., 2022; Rasmussen et al., 1992). This indicates that β-sheet assembly might be different with the presence or absence of disulphide bonds during fibril formation. Also, longer fibrils might be a result of different endpoints of the fibril formation reaction (Leonil et al., 2008). However, it is necessary to consider other factors that may influence the fibril formation reaction, for example, the initial concentration of κ-CN, the reaction temperature and pH (Thorn et al., 2014). In addition, our results indicate a possible difference in β-sheet packing between UG κ-CN B and 2G κ-CN B. TEM results show that amyloid fibrils formed in the 2G κ-CN B sample incubated at 37 °C appear narrower than UG κ-CN B incubated at 37°, possibly due to the relatively higher negative charge of 2G κ-CN B allowing a closer packing of the β-sheets or relating to the possible dissociation and repacking of aggregated proteins into a different and narrower confirmation, as suggested by Ecroyd et al. (2008). Moreover, the amyloid fibrils of the 2G κ-CN B sample appear relatively longer than those of the UG κ-CN B, sample, which might be due to the relatively faster amyloid formation rate of the 2G κ-CN B, hence longer fibrils were achieved at the point where the reaction was ceased. In UG κ-CN B, the diameter of oligomeric aggregates before incubation was similar to the width of amyloid fibrils after incubation, indicating that there is likely a link between β-sheet packing in the unglycosylated form of κ-CN B and the individual oligomeric aggregates.

The results of this study demonstrate that the rate of amyloid fibril formation and the morphology of fibrils differ between UG κ-CN B and 2G κ-CN B, implying that the presence or absence of glycans can alter the fibril formation reaction, while amyloid fibril formation rates appear to be significantly higher in 2G κ-CN B compared to UG κ-CN B. Moreover, morphology studies indicate that there may be differences in the mechanism for fibril formation with glycosylation level. Therefore, the results of the study suggest that unglycosylated κ-CN plays an important role in stabilising κ-CN, while allowing more reactive and relatively unstable glycosylated κ-CN to maintain the functional properties of the κ-CN.

5. Conclusions

Results show that amyloid fibril formation can occur at concentrations below the critical micelle concentration of κ-CN B, indicating that disassociated forms are likely the fibril formation precursors for κ-CN B at low protein concentrations. However, fibril formation was not observed in very dilute protein solutions, for example the 0.11 and 0.05 mg mL^{-1} samples prepared using 2G κ-CN B and 0.22, 0.11 and 0.05 mg mL^{-1} for UG κ-CN B. There was no significant size difference between the micelle-like self-assembled aggregate of UG and 2G κ-CN B at room temperature, indicating that glycan attachment does not influence the oligomeric arrangement of κ-CN B. Though there was no difference in the wavelength of maximum fluorescence intensity (λ_{max}), a difference in maximum fluorescence intensity (I_{max}) indicates that glycan

attachment influences the secondary or quaternary conformation of native κ-CN B. Both UG and 2G κ-CN B were able to form amyloid fibrils at 37 °C under moderate ionic strength and natural pH, however the increase in amyloid fibril formation rate with protein concentration was significantly higher for 2G κ-CN B compared to UG κ-CN B, indicating that glycan attachment influences the susceptibility of κ-CN B to form fibrils. It is suggested the ratio of the glycosylated κ-CN B to unglycosylated κ-CN B plays an important role in balancing the functional role for safe delivery of the milk from mother to neonate. The present results may also indicate differences in β-sheet packing between the two glycoforms, and more experiments employing techniques such as nuclear magnetic resonance spectroscopy, circular dichroism spectroscopy and fourier transform infrared spectroscopy can be conducted to further explore molecular packing differences with glycan attachment.

CRediT authorship contribution statement

Barana Hewa Nadugala: Contribution is over 51% including, Conceptualization, Methodology, Investigation, Visualization, and, Writing – original draft. **Rick Hantink:** Conceptualization, Methodology, Investigation. **Tom Nebl:** Methodology, Investigation. **Jacinta White:** Methodology, Investigation. **Charles N. Pagel:** Supervision, Resources, Writing – review & editing. **C.S. Ranadheera:** Supervision, Resources, Writing – review & editing. **Amy Logan:** Supervision, Resources, Formal analysis, Writing – review & editing. **Jared K. Raynes:** Conceptualization, Methodology, Supervision, Resources, Formal analysis, Writing – review & editing.

Declaration of competing interest

The authors declare the following financial interests/personal relationships which may be considered as potential competing interests:

Barana Hewa Nadugala reports administrative support was provided by No Conflict of interests. C S Ranadheera reports a relationship with Nothing to disclose that includes: funding grants. Nothing to disclose has patent Nothing to disclose pending to Nothing to disclose. The authors declare that they have no known competing financial interests or personal relationships that could have appeared to influence the work reported in this paper.

Data availability

The data that has been used is confidential.

Acknowledgment

The authors would like to thank Dr Roderick Williams, Dr Adil Malik and Mr Sean Moore (CSIRO), for their general laboratory help, Mrs Rangika Weerakkody and Dr Tanoj Singh (CSIRO) for help with the HPLC analysis, and Dr Jo Caine (CSIRO) for help with the protein purification. The authors would like to acknowledge CSIRO's 'Active Integrated Matter' (AIM) Future Science Platform, Australia, Sri Lanka Science and Technology Human Resources Development (STHRD) Project of the Asian Development Bank and the University of Melbourne Research Scholarship for supporting this project.

References

Bern, M., Caval, T., Kil, Y.J., Tang, W., Becker, C., Carlson, E., Kletter, D., Sen, K.I., Galy, N., Hagemans, D., Franc, V., Heck, A.J.R., 2018. Parsimonious charge deconvolution for native mass spectrometry. J. Proteome Res. 17 (3), 1216–1226. https://doi.org/10.1021/acs.jproteome.7b00839.

Bobe, G., Beitz, D.C., Freeman, A.E., Lindberg, G.L., 1998. Separation and quantification of bovine milk proteins by reversed-phase high-performance liquid chromatography. J. Agric. Food Chem. 46 (2), 458–463. https://doi.org/10.1021/jf970499p.

Bonfatti, V., Chiarot, G., Carnier, P., 2014. Glycosylation of κ-casein: genetic and nongenetic variation and effects on rennet coagulation properties of milk. J. Dairy Sci. 97 (4), 1961–1969. https://doi.org/10.3168/jds.2013-7418.

Bonfatti, V., Grigoletto, L., Cecchinato, A., Gallo, L., Carnier, P., 2008. Validation of a new reversed-phase high-performance liquid chromatography method for separation and quantification of bovine milk protein genetic variants. J. Chromatogr. A 1195 (1–2), 101–106. https://doi.org/10.1016/j.chroma.2008.04.075.

Bordin, G., Cordeiro Raposo, F., de la Calle, B., Rodriguez, A.R., 2001. Identification and quantification of major bovine milk proteins by liquid chromatography. J. Chromatogr. A 928 (1), 63–76. https://doi.org/10.1016/S0021-9673(01)01097-4.

Broncel, M., Falenski, J.A., Wagner, S.C., Hackenberger, C.P.R., Koksch, B., 2010. How post-translational modifications influence amyloid formation: a systematic study of phosphorylation and glycosylation in model peptides. Chem. Eur J. 16 (26), 7881–7888. https://doi.org/10.1002/chem.200902452.

Chiti, F., Dobson, C.M., 2006. Protein misfolding, functional amyloid, and human disease. Annu. Rev. Biochem. 75, 333–366. https://doi.org/10.1146/annurev.biochem.75.101304.123901.

Chun, J., Bhak, G., Lee, S.-G., Lee, J.H., Lee, D., Char, K., Paik, S.R., 2012. κ-casein-based hierarchical suprastructures and their use for selective temporal and spatial control over neuronal differentiation. Biomacromolecules 13 (9), 2731–2738. https://doi.org/10.1021/bm300692k.

Day, L., Williams, R.P.W., Otter, D., Augustin, M.A., 2015. Casein polymorphism heterogeneity influences casein micelle size in milk of individual cows. J. Dairy Sci. 98 (6), 3633–3644. https://doi.org/10.3168/jds.2014-9285.

De Kruif, C.G., 1998. Supra-aggregates of casein micelles as a prelude to coagulation. J. Dairy Sci. 81 (11), 3019–3028. https://doi.org/10.3168/jds.S0022-0302(98)75866-7.

Dobson, C.M., 2003. Protein folding and misfolding. Nature 426 (6968), 884–890. https://doi.org/10.1038/nature02261.

Ecroyd, H., Koudelka, T., Thorn, D.C., Williams, D.M., Devlin, G., Hoffmann, P., Carver, J.A., 2008. Dissociation from the oligomeric state is the rate-limiting step in fibril formation by κ-casein. J. Biol. Chem. 283 (14), 9012–9022. https://doi.org/10.1074/jbc.m709928200.

Ecroyd, H., Thorn, David C., Liu, Y., Carver, John A., 2010. The dissociated form of κ-casein is the precursor to its amyloid fibril formation. Biochem. J. 429 (2), 251–260. https://doi.org/10.1042/BJ20091949.

Farrell, H.M., Cooke, P.H., King, G., Hoagland, P.D., Groves, M.L., Kumosinski, T.F., Chu, B., 1996. Particle sizes of casein submicelles and purified κ-casein. In: Parris, N., Kato, A., Creamer, L.K., Pearce, J. (Eds.), Macromolecular Interactions in Food Technology, vol. 650. American Chemical Society, Washington DC, pp. 61–79.

Farrell, H.M., Jimenez-Flores, R., Bleck, G.T., Brown, E.M., Butler, J.E., Creamer, L.K., Hicks, C.L., Hollar, C.M., Ng-Kwai-Hang, K.F., Swaisgood, H.E., 2004. Nomenclature of the proteins of cows' milk - sixth revision. J. Dairy Sci. 87 (6), 1641–1674. https://doi.org/10.3168/jds.S0022-0302(04)73319-6.

Farrell Jr., H.M., Cooke, P.H., Wickham, E.D., Piotrowski, E.G., Hoagland, P.D., 2003. Environmental influences on bovine κ-casein: reduction and conversion to fibrillar (amyloid) structures. J. Protein Chem. 22 (3), 259–273. https://doi.org/10.1023/A:1025020503769.

Gorinstein, S., Goshev, I., Moncheva, S., Zemser, M., Weisz, M., Caspi, A., Libman, I., Lerner, H.T., Trakhtenberg, S., Martín-Belloso, O., 2000. Intrinsic tryptophan fluorescence of human serum proteins and related conformational changes. J. Protein Chem. 19 (8), 637–642. https://doi.org/10.1023/A:1007192017291.

Hamada, D., Dobson, C.M., 2002. A kinetic study of beta-lactoglobulin amyloid fibril formation promoted by urea. Protein Sci. 11 (10), 2417–2426. https://doi.org/10.1110/ps.0217702.

Hellmann, N., Schneider, D., 2019. Hands on: using tryptophan fluorescence spectroscopy to study protein structure. In: Kister, A.E. (Ed.), Protein Supersecondary Structures: Methods and Protocols. Springer, New York, pp. 379–401. https://doi.org/10.1007/978-1-4939-9161-7_20.

Hernández-Hernández, O., Lebrón-Aguilar, R., Quintanilla-López, J.E., Sanz, M.L., Moreno, F.J., 2011. Detection of two minor phosphorylation sites for bovine κ-casein macropeptide by reversed-phase liquid chromatography–tandem mass spectrometry. J. Agric. Food Chem. 59 (20), 10848–10853. https://doi.org/10.1021/jf203089n.

Hewa Nadugala, B., Pagel, C.N., Raynes, J.K., Ranadheera, C.S., Logan, A., 2022. The effect of casein genetic variants, glycosylation and phosphorylation on bovine milk protein structure, technological properties, nutrition and product manufacture. Int. Dairy J. 133, 105440 https://doi.org/10.1016/j.idairyj.2022.105440.

Hill, R.D., 1963. The preparation of κ-casein. J. Dairy Res. 30 (1), 101–107. https://doi.org/10.1017/S0022029900011304.

Hirs, C.H.W., 1967. Reduction and S-carboxymethylation of proteins. In: Hirs, C.H.W. (Ed.), Methods in Enzymology, vol. 11. Academic Press, Cambridge, pp. 199–203. https://doi.org/10.1016/S0076-6879(67)11022-7.

Holland, J.W., Deeth, H.C., Alewood, P.F., 2006. Resolution and characterisation of multiple isoforms of bovine κ-casein by 2-DE following a reversible cysteine-tagging enrichment strategy. Proteomics 6 (10), 3087–3095. https://doi.org/10.1002/pmic.200500780.

Holt, C., Carver, J.A., Ecroyd, H., Thorn, D.C., 2013. Invited review: caseins and the casein micelle: their biological functions, structures, and behavior in foods. J. Dairy Sci. 96 (10), 6127–6146. https://doi.org/10.3168/jds.2013-6831.

Horne, D.S., 2003. Casein micelles as hard spheres: limitations of the model in acidified gel formation. Colloids Surf., A 213 (2–3), 255–263. https://doi.org/10.1016/s0927-7757(02)00518-6.

Hudson, S.A., Ecroyd, H., Kee, T.W., Carver, J.A., 2009. The thioflavin T fluorescence assay for amyloid fibril detection can be biased by the presence of exogenous compounds. FEBS J. 276 (20), 5960–5972. https://doi.org/10.1111/j.1742-4658.2009.07307.x.

Jensen, H.B., Holland, J.W., Poulsen, N.A., Larsen, L.B., 2012. Milk protein genetic variants and isoforms identified in bovine milk representing extremes in coagulation properties. J. Dairy Sci. 95 (6), 2891–2903. https://doi.org/10.3168/jds.2012-5346.

Jensen, H.B., Pedersen, K.S., Johansen, L.B., Poulsen, N.A., Bakman, M., Chatterton, D.E. W., Larsen, L.B., 2015. Genetic variation and posttranslational modification of bovine κ-casein: effects on caseino-macropeptide release during renneting. J. Dairy Sci. 98 (2), 747–758. https://doi.org/10.3168/jds.2014-8678.

Krebs, M.R.H., Morozova-Roche, L.A., Daniel, K., Robinson, C.V., Dobson, C.M., 2004. Observation of sequence specificity in the seeding of protein amyloid fibrils. Protein Sci. 13 (7), 1933–1938. https://doi.org/10.1110/ps.04707004.

Kreuß, M., Strixner, T., Kulozik, U., 2009. The effect of glycosylation on the interfacial properties of bovine caseinomacropeptide. Food Hydrocolloids 23 (7), 1818–1826. https://doi.org/10.1016/j.foodhyd.2009.01.011.

Leonil, J., Henry, G., Jouanneau, D., Delage, M.-M., Forge, V., Putaux, J.-L., 2008. Kinetics of fibril formation of bovine κ-casein indicate a conformational rearrangement as a critical step in the process. J. Mol. Biol. 381 (5), 1267–1280. https://doi.org/10.1016/j.jmb.2008.06.064.

Mercier, J.-C., Brignon, G., Ribadeau-dumas, B., 1973. Structure primaire de la caséine κB bovine. Eur. J. Biochem. 35 (2), 222–235. https://doi.org/10.1111/j.1432-1033.1973.tb02829.x.

Nwosu, C.C., Strum, J.S., An, H.J., Lebrilla, C.B., 2010. Enhanced detection and identification of glycopeptides in negative ion mode mass spectrometry. Anal. Chem. 82 (23), 9654–9662. https://doi.org/10.1021/ac101856r.

O'Riordan, N., Kane, M., Joshi, L., Hickey, R.M., 2014. Structural and functional characteristics of bovine milk protein glycosylation. Glycobiology 24 (3), 220–236. https://doi.org/10.1093/glycob/cwt162.

Pan, K., Zhong, Q., 2015. Amyloid-like fibrils formed from intrinsically disordered caseins: physicochemical and nanomechanical properties. Soft Matter 11 (29), 5898–5904. https://doi.org/10.1039/C5SM01037C.

Perutz, M.F., Johnson, T., Suzuki, M., Finch, J.T., 1994. Glutamine repeats as polar zippers: their possible role in inherited neurodegenerative diseases. Proc. Natl. Acad. Sci. USA 91 (12), 5355–5358. https://doi.org/10.1073/pnas.91.12.5355.

Rambaran, R.N., Serpell, L.C., 2008. Amyloid fibrils: abnormal protein assembly. Prion 2 (3), 112–117. https://doi.org/10.4161/pri.2.3.7488.

Rasmussen, L.K., Højrup, P., Petersen, T.E., 1992. The multimeric structure and disulfide-bonding pattern of bovine κ-casein. Eur. J. Biochem. 207 (1), 215–222. https://doi.org/10.1111/j.1432-1033.1992.tb17040.x.

Raynes, J.K., Day, L., Augustin, M.A., Carver, J.A., 2015. Structural differences between bovine A1 and A2 β-casein alter micelle self-assembly and influence molecular chaperone activity. J. Dairy Sci. 98 (4), 2172–2182. https://doi.org/10.3168/jds.2014-8800.

Raynes, J.K., Day, L., Crepin, P., Horrocks, M.H., Carver, J.A., 2017. Coaggregation of kappa-Casein and beta-Lactoglobulin produces morphologically distinct amyloid fibrils. Small 13 (14). https://doi.org/10.1002/smll.201603591.

Raynes, J.K., Vincent, D., Zawadzki, J.L., Savin, K., Mertens, D., Logan, A., Williams, R.P. W., 2018. Investigation of age gelation in UHT milk. Beverages 4 (4), 21. https://doi.org/10.3390/beverages4040095. Article 95.

Saito, T., Itoh, T., 1992. Variations and distributions of o-glycosidically linked sugar chains in bovine κ-casein. J. Dairy Sci. 75 (7), 1768–1774. https://doi.org/10.3168/jds.S0022-0302(92)77936-3.

Schedin-Weiss, S., Winblad, B., Tjernberg, L.O., 2014. The role of protein glycosylation in Alzheimer disease. FEBS J. 281 (1), 46–62. https://doi.org/10.1111/febs.12590.

Schlunegger, M.P., Bennett, M.J., Eisenberg, D., 1997. Oligomer formation by 3D domain swapping: a model for protein assembly and misassembly. Adv. Protein Chem. 50, 61–122. https://doi.org/10.1016/s0065-3233(08)60319-8.

Segers-Nolten, I., van Raaij, M., Subramaniam, V., 2011. Biophysical analysis of amyloid formation. In: Ducheyne, P. (Ed.), Comprehensive Biomaterials. Elsevier, Oxford, pp. 347–359. https://doi.org/10.1016/B978-0-08-055294-1.00086-6.

Sipe, J.D., Benson, M.D., Buxbaum, J.N., Ikeda, S.-i., Merlini, G., Saraiva, M.J.M., Westermark, P., 2016. Amyloid fibril proteins and amyloidosis: chemical identification and clinical classification International Society of Amyloidosis 2016 nomenclature guidelines. Amyloid 23 (4), 209–213. https://doi.org/10.1080/13506129.2016.1257986.

Sunde, M., Serpell, L.C., Bartlam, M., Fraser, P.E., Pepys, M.B., Blake, C.C.F., 1997. Common core structure of amyloid fibrils by synchrotron X-ray diffraction. J. Mol. Biol. 273 (3), 729–739. https://doi.org/10.1006/jmbi.1997.1348.

Thorn, D.C., Ecroyd, H., Carver, J.A., 2014. Polymorphism in casein protein aggregation and amyloid fibril formation. In: Uversky, V.N., Lyubchenko, Y.L. (Eds.), Bio-nanoimaging. Academic Press, Boston, pp. 323–331.

Thorn, D.C., Meehan, S., Sunde, M., Rekas, A., Gras, S.L., MacPhee, C.E., Dobson, C.M., Wilson, M.R., Carver, J.A., 2005. Amyloid fibril formation by bovine milk κ-casein and its inhibition by the molecular chaperones αs- and β-casein. Biochemistry 44 (51), 17027–17036. https://doi.org/10.1021/bi051352r.

Vincent, D., Elkins, A., Condina, M.R., Ezernieks, V., Rochfort, S., 2016. Quantitation and identification of intact major milk proteins for high-throughput LC-ESI-Q-TOF MS analyses. PLoS One 11 (10), e0163471. https://doi.org/10.1371/journal.pone.0163471.

Vivian, J.T., Callis, P.R., 2001. Mechanisms of tryptophan fluorescence shifts in proteins. Biophys. J. 80 (5), 2093–2109. https://doi.org/10.1016/s0006-3495(01)76183-8.

Vreeman, H.J., Visser, S., Slangen, C.J., Van Riel, J.A., 1986. Characterization of bovine kappa-casein fractions and the kinetics of chymosin-induced macropeptide release from carbohydrate-free and carbohydrate-containing fractions determined by high-performance gel-permeation chromatography. Biochem. J. 240 (1), 87–97.

Walstra, P., 1999. Casein sub-micelles: do they exist? Int. Dairy J. 9 (3), 189–192. https://doi.org/10.1016/S0958-6946(99)00059-X.

Waugh, D.F., 1958. The interactions of αs-β- and κ-caseins in micelle formation. Discuss. Faraday Soc. 25, 186–192. https://doi.org/10.1039/df9582500186.

Wetzel, R., 2013. Amyloid. In: Lennarz, W.J., Lane, M.D. (Eds.), Encyclopedia of Biological Chemistry, second ed. Academic Press, Waltham, pp. 100–104. https://doi.org/10.1016/B978-0-12-378630-2.00167-5.